Thermal-transport properties of CeNiSn

S. Paschen, B. Wand, G. Sparn, and F. Steglich
MPI for Chemical Physics of Solids, Nöthnitzer Strasse 40, D-01187 Dresden, Germany

Y. Echizen and T. Takabatake
Department of Quantum Matter, ADSM, Hiroshima University, Kagamiyama 1-3-1, Higashi-Hiroshima 739-8526, Japan
(Received 17 July 2000)

We present thermal-conductivity κ and thermopower S measurements on high-quality single crystalline CeNiSn along the three crystallographic axes a, b, and c in the temperature range between 100 mK and 7 K and in magnetic fields up to 8 T applied along the a axis. Both κ and S are highly anisotropic. However, characteristic features that may be attributed to the opening of a pseudogap in the electronic density of states (DOS) at the Fermi energy η below 10 K are seen for *all* three crystallographic directions. These features are strongly suppressed by a magnetic field of 8 T applied along the a axis. At the lowest temperatures we have evidence for the presence of a residual metallic DOS at η, again for all three directions. The saturation of the reduced Lorenz number L/L_0 to a value distinctly higher than one is an interesting feature which deserves further investigation.

I. INTRODUCTION

Since the discovery of CeNiSn in 1984[1] and the claim[2] that CeNiSn is one of the rare examples of valence-fluctuating cerium compounds with an energy pseudogap in the electronic density of states (DOS) at the Fermi level η, hundreds of reports on both experimental and theoretical aspects of this compound have appeared in the literature. One reason for the strong interest in CeNiSn is the special role it was claimed[3] to play among the so-called Kondo insulators,[3] systems in which the hybridization of a flat $4f$ band with a broad conduction band is believed to lead, at half band filling, to the formation of a narrow gap surrounded by states with predominant $4f$ character. CeNiSn was reported to have the smallest energy gap and to be, together with the isostructural compound CeRhSb, the only noncubic representative of this interesting class of strongly correlated semiconductors.

According to a single-crystal x-ray diffraction study[4] CeNiSn crystallizes in the orthorhombic non-centrosymmetric space group $Pn2_1a$. However, from neutron diffraction experiments[5] it was claimed that the structure of CeNiSn is sufficiently well described by the centrosymmetric space group $Pnma$. For both cases, the structure may be described as two-dimensional Ce-Ni-Sn networks parallel to the ac plane stacked along the b direction. Alternatively, the structure may be viewed as a stacking sequence of two-dimensional Ce networks parallel to the bc plane with a Ni-Sn puckered network between them. This will result in anisotropic interactions of the almost localized $4f$ electrons of Ce with the delocalized conduction electrons and therefore in anisotropic magnetic and transport properties, as was already noted by Takabatake *et al.*[6]

So far, most emphasis was put on the investigation of the pseudogap. Evidence for its opening at temperatures of the order of 10 K is, for example, derived from NMR measurements of the spin-lattice relaxation rate $1/T_1$,[7] from tunneling experiments,[8] and from measurements of the ESR linewidth.[9] Our main interest in the present work, however, concerns a potential residual DOS within the pseudogap, information on which may be obtained by measurements at very low temperatures only. NMR measurements of $1/T_1$ vs T revealed a Korringa law,[10] and specific-heat measurements a linear temperature dependence,[11] both below approximately 500 mK. This is evidence for a finite DOS at the Fermi level. A more recent measurement of the specific heat gave a slightly different result.[12] The ratio of the electronic specific heat to the temperature, $C_{\rm el}/T$, was reported to slightly increase with decreasing temperature below 500 mK. From this it was inferred that the DOS of CeNiSn has a peak at the Fermi level inside the pseudogap. As we shall show below, thermal-transport measurements at very low temperatures are a valuable tool for extracting additional information on this residual DOS. In particular, measurements along the three crystallographic axes provide information on the anisotropy of the residual charge-carrier density.

II. SAMPLES AND EXPERIMENTAL SETUP

The single crystalline CeNiSn samples investigated here were grown by a Czochralski method using a radio-frequency furnace and were subsequently purified by the technique of solid-state electro-transport (SSE). Details of the crystal growth and purification process have been described in Refs. 13 and 14. Rods elongated along the a, b, and c axes were cut by spark erosion to the dimensions $4.7\times0.91\times0.77$ mm^3, $5.31\times0.78\times0.65$ mm^3, and $5.45\times0.84\times0.69$ mm^3, respectively. The thermal conductivity and the thermopower were measured by the usual steady-state methods in the temperature range between 100 mK and 7 K in magnetic fields up to 8 T. In all cases the magnetic field was applied along the a axis, which is the easy axis of magnetization.[6] Further experimental details are given in Ref. 15. The electrical resistivity of the a-axis crystal was measured by a standard low-frequency lock-in technique. On the a-axis crystal thermal conductivity and electrical resistivity were measured with the same spot-welded contacts.

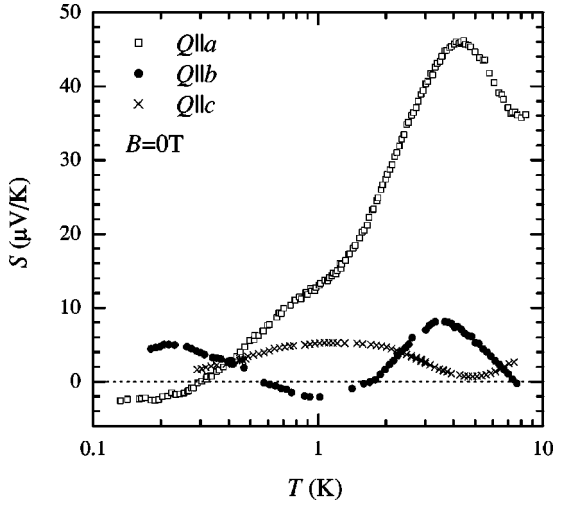

FIG. 1. Thermopower S of CeNiSn along the three crystallographic axes a, b, and c vs temperature T.

This is essential for a quantitative analysis of the reduced Lorenz number to be presented below.

III. EXPERIMENTAL RESULTS

In this section we present our data and compare them to data available in the literature. For more clarity our interpretation and discussion is kept for the next section. The thermopower S of CeNiSn measured along the a, b, and c axes is shown in Fig. 1 as a function of temperature T between 100 mK and 7 K. $S(T)$ is highly anisotropic. The largest values are found for $S_a(T)$, which passes over a maximum of 48 μV/K at 4.4 K. This maximum is six times larger than the maximum observed for $S_b(T)$ at 3.5 K, and nine times larger than the maximum of $S_c(T)$ at 1 K. The $S(T)$ behavior at the lowest temperatures is extremely rich, with several well-defined structures, particularly for the a- and b-axis crystals, where $S(T)$ changes sign once and twice, respectively. Our data differ from the published data[6,14,16–18] on other single-crystalline CeNiSn samples in several respects. First, all previous reports give a higher low-temperature maximum for the c axis than for the a axis. Our results, however, yield the largest maximum for the a axis. In the temperature range where the low-temperature maximum in $S_c(T)$ is reported in the literature (2 to 3 K), our $S_c(T)$ data display no maximum at all, but are small and vary smoothly instead. Secondly, the temperature of the maximum of our $S_a(T)$ data is by at least 1 K higher than in all other reports. Thirdly, a maximum at approximately 3.5 K in $S_b(T)$ as seen in our data was reported only in Ref. 14, while Refs. 6 and 18 report a minimum instead. Below 1.5 K, comparison can be made only with the data of Ref. 16. Here, $S(T)$ was reported to be proportional to T below 1 K, in striking contrast with our findings. All these discrepancies are most probably related to the differences in sample quality. As mentioned above, none of the single crystals on which $S(T)$ measurements were reported so far[6,14,16–18] was purified by the SSE technique but, as was shown by Nakamoto *et al.*,[14] this treatment is crucial for improving the sample quality. The SSE-treated samples investigated here have by far the lowest resistivity at 2 K and are the only ones with a positive slope $d\rho/dT$ at 2 K, clear indications for the highest sample quality.

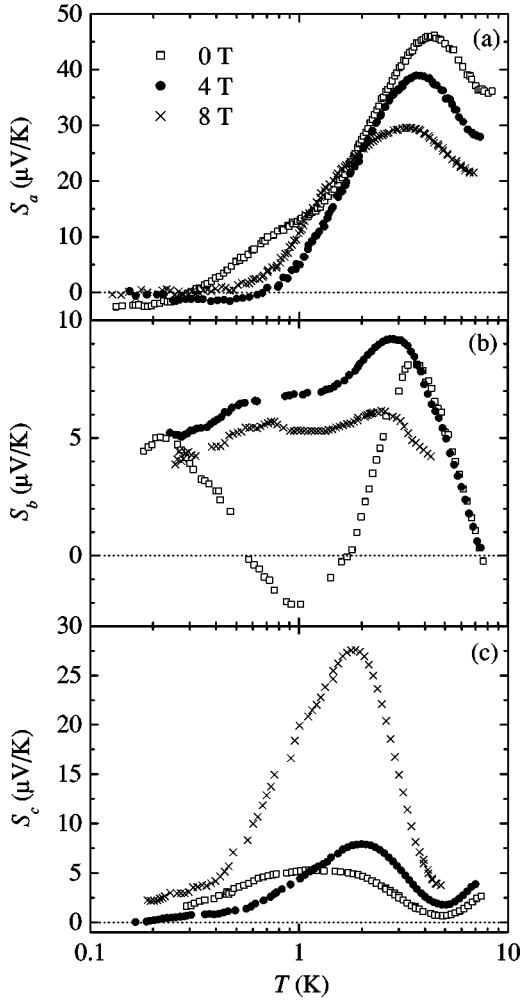

FIG. 2. Temperature dependence of the thermopower $S(T)$ of CeNiSn along the a, b, and c axis in panels (a), (b), and (c), respectively, each in zero magnetic field and at 4 and 8 T. The field was applied along the a axis.

Figure 2 shows semilogarithmic plots of $S_a(T)$, $S_b(T)$, and $S_c(T)$ in magnetic fields of 0, 4, and 8 T applied along the a axis. For all three directions a magnetic field affects the thermopower drastically. For $S_a(T)$, the maximum at 4.4 K is reduced in size and shifted to lower temperatures. Also the shoulder at approximately 1 K is suppressed by the field. In the b direction, the minimum at 1 K is already suppressed by 4 T. This leads to an increase of the maximum at 3.5 K, but a field of 8 T overcompensates this effect and clearly reduces the size of this maximum and shifts it to lower temperatures, as was also observed for the a direction. The behavior of $S_c(T)$, however, is completely different. Here, the maximum at 1 K is strongly enhanced and shifted to higher temperatures by the magnetic field. Magnetic-field measurements were done only in Refs. 16 and 18 where the field was applied along and perpendicular to the heat flow, respectively. The results for $S_a(T,B=8\ \mathrm{T}\|a)$ of Ref. 16 are in qualitative agreement with our data. At 8 T, the maximum of $S_a(T,B=0\ \mathrm{T})$ at 3.5 K is reduced by 50% and shifted to lower temperatures by 1 K. The $S_c(T,B\|a)$ data of Ref. 18, however, are in striking contrast with our data. While the peak in

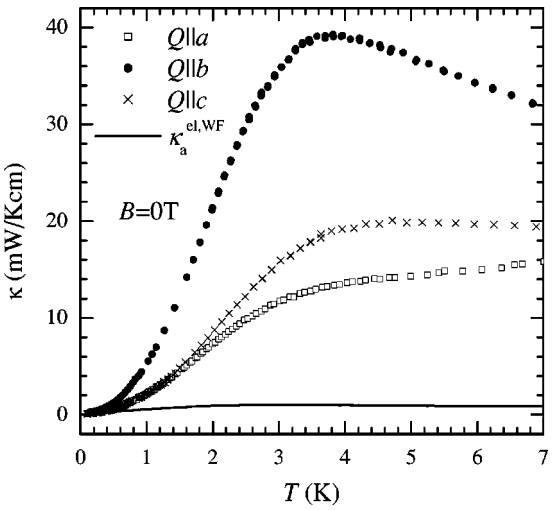

FIG. 3. Thermal conductivity κ of CeNiSn along the three crystallographic axes a, b, and c vs temperature T. The solid curve represents the electronic thermal conductivity along the a axis obtained from the Wiedemann-Franz (WF) law.

$S_c(T,B=0$ T) at 2.3 K is completely *suppressed* by 8 T in Ref. 18, in our sample the magnetic field *creates* a peak centered at approximately 2 K. The $S_b(T,B\|a)$ data of Ref. 18 are difficult to compare with our data since already the zero-field data are very different from ours.

In Fig. 3 we present the thermal conductivity κ of CeNiSn measured along the a, b, and c axes as a function of temperature T between 100 mK and 7 K. Similar to $S(T)$, $\kappa(T)$ is highly anisotropic. However, for *all* three directions anomalous enhancements of κ are observed in the investigated temperature range. The highest values are found for $\kappa_b(T)$, which shows a pronounced anomaly with a maximum of almost 40 mW/Kcm at 3.8 K. For $\kappa_c(T)$ a very shallow maximum of 20 mW/K cm is found at approximately 5 K. For $\kappa_a(T)$ a plateau at 4.5 K is found. Again we compare our data with published $\kappa(T)$ data on other CeNiSn single crystals in the temperature range 100 mK to 8 K (Ref. 16) (a and c axis only), 1.6 to 18 K,[19] and 1.5 to 100 K.[20] There is at least qualitative agreement between all reports: The largest anomaly is observed for the b direction, smaller anomalies are found for $\kappa_a(T)$ and $\kappa_c(T)$. A quantitative comparison shows that for our sample the maximum of $\kappa_b(T)$ is almost twice as high as for the previous samples. In addition, this maximum occurs at a temperature more than 1 K lower than reported in the literature.[16,19,20] The higher thermal conductivity confirms that among all samples studied so far, the SSE-treated ones are of the highest quality.

Application of a magnetic field parallel to the a axis leads to a reduction of the above discussed enhancements in $\kappa(T)$ for all three directions, as is shown in Fig. 4. The effect is strongest for the b direction, where a magnetic field of 8 T reduces κ at 3.8 K, the temperature of the maximum, by almost 50%. The same field reduces $\kappa_a(T)$ and $\kappa_c(T)$ by 30 and 35% at 4.5 and 5 K, respectively. This is in overall agreement with literature results on other CeNiSn single crystals. A field of 8 T applied along the a axis was found to reduce $\kappa_a(T)$ by 25% at 5 K (Ref. 16) and by almost 30% at 4.3 K,[20] in good agreement with our results. However, the depression by about 30% of $\kappa_b(T)$ of the sample addressed in Ref. 20 by the same field is distinctly smaller than for our sample.

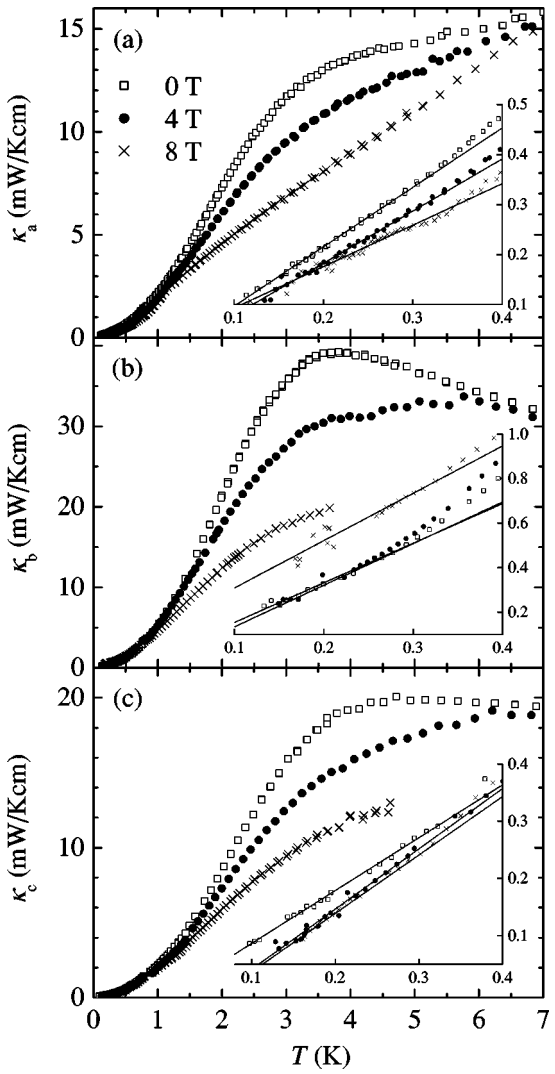

FIG. 4. Temperature dependence of the thermal conductivity $\kappa(T)$ of CeNiSn along the a, b, and c axis in panels (a), (b), and (c), respectively, each in zero magnetic field and at 4 and 8 T. The field was applied along the a axis. The insets show closeups at low temperatures. The lines are best linear fits to the data.

The electrical resistivity of the a-axis crystal is shown in the inset of Fig. 5 as a function of temperature between 100 mK and 7 K. As mentioned above, the sample and its electrical contacts are the same as used for the thermal-conductivity measurement. The metallic behavior down to the lowest temperatures confirms the high sample quality. The electrical resistivities of the b- and c-axis crystals in the temperature range 400 mK to 300 K have been published previously.[21]

IV. ANALYSIS AND DISCUSSION

We begin with a discussion of the thermopower. Usually, distinction is made between the diffusion thermopower S_d and several drag contributions. The phonon-drag thermopower frequently leads to a maximum in $S(T)$ at 0.1 to $0.2\times\Theta_D$, where Θ_D is the Debye temperature. From specific-heat measurements on LaNiSn, Θ_D of CeNiSn was

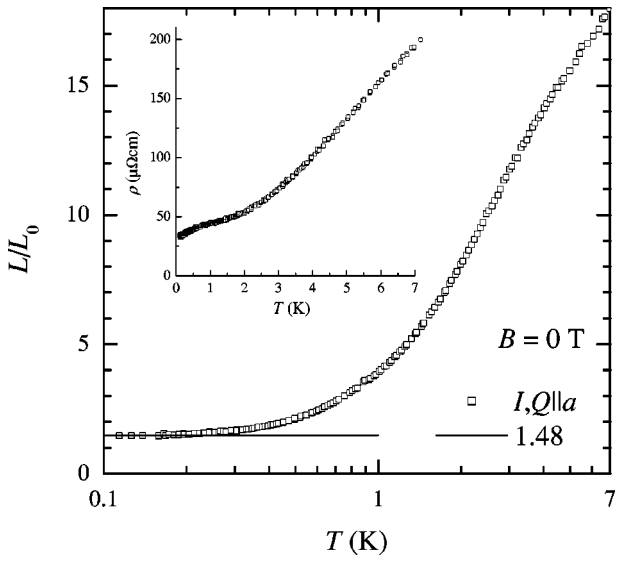

FIG. 5. Reduced Lorenz number L/L_0 of CeNiSn along the *a* axis as a function of temperature *T*. The inset shows the temperature dependence of the electrical resistivity $\rho(T)$ of the same crystal measured along the *a* axis.

estimated[22] to be 230 K. Thus, the phonon-drag peak in $S(T)$ is expected to lie outside the temperature range investigated here. Since spin fluctuations are believed to be important in CeNiSn, a paramagnon-drag thermopower may be expected. In many paramagnetic spin-fluctuation systems extrema in $S(T)$ have been observed near the spin-fluctuation temperature.[23] Inelastic neutron-scattering measurements[24,25] revealed two excitations at 2 and 4 meV below approximately 20 K. These were interpreted as three-dimensional and quasi one-dimensional dynamic antiferromagnetic correlations, respectively. It may well be possible that at least part of the anomalies found in the thermopower at approximately 20 K (Refs. 6, 13, 17, and 18) is due to the paramagnon drag from these fluctuations. Since there is no obvious reason to assume that drag contributions are important at much lower temperatures, i.e., below 7 K, we restrict ourselves to an interpretation of our data in terms of a diffusion thermopower.

For a degenerate Fermi gas the diffusion thermopower is, in the Sommerfeld derivation, given by the so-called Mott expression[26] $S_d = \pi^2 k_B^2/(3e) T(\partial \ln \sigma/\partial \epsilon)_{\epsilon=\eta}$, where σ is the electrical conductivity, η the Fermi energy, *e* the elementary charge including sign, and the other symbols have their usual meaning. At $T=0$, $S_d=0$. If $(\partial \ln \sigma/\partial \epsilon)_{\epsilon=\eta}$ is temperature independent, S_d is linear in *T*. In heavy-fermion systems, the electronic quasiparticles defined in a one-band model of itinerant fermions are complex objects, i.e., they are dominated by the local *f* degrees of freedom, with an admixture of itinerant conduction-electron contributions.[27] In a few heavy-fermion metals, both ''heavy'' and ''light'' charge carriers have, in fact, been identified via low-temperature de Haas–van Alphen measurements on different parts of the renormalized Fermi surface.[28] As was shown by Zwicknagl,[27] the large T^2 term in $\rho(T)$ found in the low-temperature regime of ''heavy Fermi liquids'' like $CeCu_6$[29] leads to the following scenario: While ''light'' charge carriers provide the electrical current, their main scatterers are the ''heavy'' ones. Adopting this point of view in analyzing the transport properties of CeNiSn which behaves like a heavy fermion above the characteristic (Kondo) temperature T^*, one may consider a two-band model.[26] In this model the thermopower is well represented by the ''light'' carriers (or ''conduction electrons'') with the DOS N_s being scattered from the ''heavy carriers'' (or ''4*f* electrons'') with a relaxation rate τ_f^{-1}. Thus, $\sigma \propto N_s \tau_f$. In a first approximation, we may set $\tau_f^{-1}(\epsilon) \propto N_f(\epsilon)$, where N_f is the resonant 4*f*-electron DOS, and obtain $S_d = \pi^2 k_B^2/(3e) T(\partial \ln N_s/\partial \epsilon - \partial \ln N_f/\partial \epsilon)_{\epsilon=\eta}$. The term $(\partial \ln N_f/\partial \epsilon)_{\epsilon=\eta}$ may reach very large absolute values compared to the corresponding expression in *d*-band metals. Pronounced temperature dependences of this term, leading to nonlinearities in $S_d(T)$, are expected at two temperature scales: at temperatures above $T^* \approx 50$ K,[22] where the so-called Abrikosov-Suhl resonance, $N_f(\epsilon)$, becomes strongly reduced, and at temperatures below 10 K where a gap opens within $N_f(\epsilon)$. It is known from Hall-effect measurements[11] that the effective charge-carrier concentration decreases steeply upon cooling below 5 to 10 K. In the two band model this means that also in the conduction-electron DOS, $N_s(\epsilon)$, a gap opens in this temperature range. Thus, below 10 K the term $(\partial \ln N_s/\partial \epsilon)_{\epsilon=\eta}$ may contribute non-negligibly to S_d. The interpretation of the $S(T)$ data below 10 K first given by Takabatake *et al.*[6] and quoted by most authors of later publications is the following. Upon cooling, the increase in $S_i(T)$ below 5 to 10 K was claimed to result from the opening of a pseudogap whereas the maxima observed at least for S_a and S_c in the vicinity of 3 K were said to suggest a residual DOS with a temperature-dependent structure. We believe that our data show that this interpretation has to be slightly modified. We shall start with the features related to the opening of the pseudogap. While both S_a and S_b increase below 8 K, S_c decreases. An increase of S_c sets in only at approximately 4.5 K. According to the above interpretation this would mean that the pseudogap in *c* direction opens at lower temperatures than the ones in *a* and *b* direction. Thermal-conductivity measurements,[20] however, indicate that the pseudogap opens at the same temperature for all three directions. Thus we propose that it is the slight decrease of S_c when cooling below 8 K which reflects the onset of the gap opening in *c* direction. The extrema in the vicinity of 4 K, i.e., the maxima of $S_a(T)$ and $S_b(T)$ and the minimum of $S_c(T)$ might correspond to $N_s(\epsilon)$ and/or $N_f(\epsilon)$ reaching the steepest slopes at this temperature. The residual DOS, on the other hand, becomes apparent only at lower temperatures. The features at 1 K, i.e., the shoulder in $S_a(T)$, the minimum in $S_b(T)$, and the maximum in $S_c(T)$ indicate that very narrow features in the DOS show up at this temperature, in agreement with the specific-heat results[12] mentioned above. We propose two explanations for this to happen. Firstly, the above-mentioned ($T^* \approx 50$ K) Abrikosov-Suhl resonance has very narrow ''side features,'' which exist at the Fermi level already well above 1 K but become apparent only at 1 K when they cease to be smeared out by the Fermi function. Secondly, a second extremely narrow many-body resonance that forms within the pseudogap of the first (wide) Abrikosov-Suhl resonance, $N_f(\epsilon)$, starts to develop only at 1 K. Finally, the appearance of a minimum in $S_a(T)$ and a maximum in $S_b(T)$ at $T \leqslant 200$ mK suggest that the

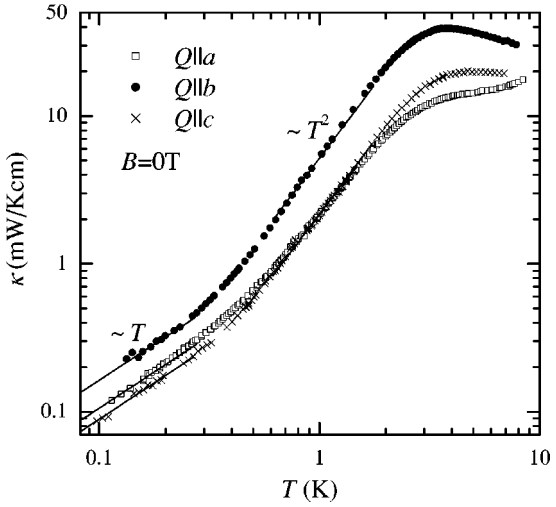

FIG. 6. Thermal conductivity κ data of Fig. 3 replotted on a double-logarithmic scale. The straight lines at low temperatures have slope one, the lines at higher temperatures slope 2.

residual DOS at the Fermi level is temperature dependent even far below 1 K. The features in $S(T)$ associated with the gap opening, which were described above, are strongly suppressed by a magnetic field applied along the *a* axis. In the Kondo lattice model a destruction of the coherence gap is expected at low magnetic-fields if the RKKY and the Kondo interaction are of similar strength.[30] That this is indeed the case for CeNiSn was very recently shown by experiments under uniaxial stress.[31] At pressures of only 0.1 GPa applied along the *b* or *c* axis, CeNiSn orders antiferromagnetically. The unusual magnetic-field dependence of the features in $S(T)$ at approximately 1 K, i.e., the suppression of the shoulder in $S_a(T)$ and of the minimum in $S_b(T)$ and the strong enhancement of the maximum in $S_c(T)$ would, in our above interpretation, indicate that the magnetic field leads to a redistribution in *k* space of the charge-carrier density giving rise to the residual DOS.

We now turn to the discussion of the thermal-conductivity data. According to the high-temperature data of Ref. 20, the thermal conductivity of CeNiSn decreases continuously when cooling from 100 K to approximately 10 K. Below this temperature unusual enhancements of $\kappa(T)$, most pronounced for the *b* axis, are observed (Fig. 3). As the authors of previous reports,[16,19,20] we believe that these enhancements result from the opening of a pseudogap. The mechanism for the enhancements will be discussed below. In addition to our $\kappa(T)$ data as measured, we have plotted in Fig. 3 the electronic contribution to the thermal conductivity along the *a* axis, $\kappa_a^{\mathrm{el,WF}}(T)$, calculated from the electrical resistivity along the *a* axis under the assumption that the Wiedemann-Franz (WF) law is valid. According to this estimate the electronic contribution is negligible above approximately 1 K. In Fig. 6 we replot the data of Fig. 3 on a double-logarithmic scale. Between 600 mK and 2 K, the $\kappa_i(T)$ data are reasonably well approximated by $\kappa \propto T^2$. A quadratic temperature dependence of $\kappa(T)$ is commonly attributed to a phononic thermal conductivity with predominant scattering of phonons from charge carriers. One assumption made in the derivation of the quadratic temperature dependence[32] is that the charge-carrier concentration is temperature independent. According to Hall-effect measurements this is, however, not entirely true for CeNiSn. At least for the *a* axis, for which the Hall coefficient R_{H} was measured down to 500 mK,[33] $|R_{\mathrm{H}}|$ does not cease to increase even at 500 mK. If R_{H} is temperature dependent, one expects[32] $\kappa(T) \propto T^2 \times (R_{\mathrm{H}}(T))^{2/3}$ which, with the $R_{\mathrm{H}}(T)$ data of Ref. 33, does indeed give a better agreement with our $\kappa_a(T)$ data than the pure $\kappa(T) \propto T^2$ law. Since our $\kappa_b(T)$ and $\kappa_c(T)$ data follow the $\kappa(T) \propto T^2$ law better than our $\kappa_a(T)$ data do, we predict that, below 2 K, R_{H} should show a weaker temperature dependence both along the *b* and *c* axis than along the *a* axis. The dominant heat carriers being phonons between 600 mK and 2 K is in agreement with $\kappa_a^{\mathrm{el,WF}} \ll \kappa_a$, as was shown in Fig. 3. The phonon mean free path l may be estimated from the relation $\kappa = Cvl/3$, where C is the lattice specific heat and v the mean phonon velocity. Using the phonon contribution $C = \beta T^3$ with $\beta = 0.49$ mJ/K^{4}mol of LaNiSn,[22] the sound velocities calculated from the elastic constants C_{11}, C_{22}, and C_{33} of CeNiSn,[34] and our $\kappa(T)$ data, we obtain $l_a = 31$ μm, $l_b = 66$ μm, and $l_c = 35$ μm at 1 K and values approximately one order of magnitude smaller at 4 K. From these values, which are much smaller than the smallest sample dimension of 0.65 mm, and from the quadratic temperature dependence of $\kappa(T)$ it is clear that the regime of boundary scattering ($\kappa \propto T^3$) is not reached at these temperatures. Instead, the phonons are strongly scattered from charge carriers. Further evidence for this scenario comes from the data below 300 mK. Here, κ is a linear function of T for all three directions. The linear-in-T dependence of κ below 300 mK suggests that in this temperature range the heat is predominantly transported by charge carriers. The existence of this electronic contribution is strong evidence for a residual charge-carrier density at the Fermi level for all three crystallographic directions. The magnetic-field dependence of the low-temperature thermal conductivity is shown in the insets of Fig. 4. While $\kappa_a(T)$ and $\kappa_c(T)$ are reduced by the magnetic field, a field of 8 T clearly enhances $\kappa_b(T)$. Next we discuss the temperature range between 2 and 7 K, where the unusual enhancements in $\kappa(T)$ related to the opening of the pseudogap are observed. First we argue that, as between 600 mK and 2 K, also in this temperature range the thermal conductivity is dominated by the phonon contribution. Even though the effective charge-carrier concentration increases strongly from 2 to 7 K,[33] the electrical conductivity *de*creases,[33] which must be due to a strongly decreasing mobility. Thus the strong increase of the charge-carrier concentration is not expected to translate into a strong increase of the electronic thermal conductivity between 2 and 7 K. In fact, the electronic thermal conductivity estimated with the help of the WF law, $\kappa^{\mathrm{el,WF}}$, is only weakly temperature dependent and small compared to the phonon thermal conductivity in the temperature range under discussion (Fig. 3). At higher temperatures, $\kappa^{\mathrm{el,WF}}$ was estimated[20] to increase continuously and to reach about 25% of the total thermal conductivity at 100 K. Our second claim is that also the dominating scattering mechanism is the same in the temperature range from 600 mK to 2 K and, at least, up to 7 K, namely phonon scattering from charge carriers. This is plausible because, as mentioned above, the number of charge carriers and therefore the number of phonon scatterers increases with increasing temperature. With these two assumptions the

enhancements[20] observed in κ upon cooling below 10 K can be explained as follows. When the gap starts to open, charge carriers start to freeze out which reduces the phonon-electron scattering rate and leads to the observed enhancements in $\kappa_i(T)$. This mechanism was already proposed by Ishikawa *et al.*[19] from the similarity of the gap-related features in CeNiSn with those in high-T_c cuprates. Our analysis provides strong evidence for this scenario. Also the field dependence is well understood in this picture. Application of magnetic fields along the *a* axis suppresses the pseudogap and thus the decrease of the charge-carrier concentration upon cooling below 10 K. Therefore the enhancements in $\kappa_i(T)$ observed in zero field are reduced at 4 and 8 T.

It is not obvious to establish a relation between the anisotropy in our data and the crystal structure of CeNiSn.[4,5] The following structural information might be relevant in this sense. The shortest Ce-Ce distances occur almost parallel (10° out of the *a* direction) to the *a* axis, such that the Ce atoms form only slightly ragged zig-zag chains in the *ac* plane along *a*. The shortest Ce-Ni distances occur in the same *ac* plane. Taking also the second and third shortest Ce-Ni distances, which are only by 1.9% and 2.3% longer, zig-zagged Ce-Ni planes are formed which are stacked along the *a* axis. Some of the properties observed in the literature are at least plausible with these structural considerations. While uniaxial pressure *p* applied along the *b* or *c* direction drives CeNiSn antiferromagnetic, $p \| a$ does not.[31] One can imagine that $p \| b$ or *c* disturbs the hybridization in the Ce-Ni planes while $p \| a$ only brings the planes closer to each other. Disturbing the hybridization may lead to the RKKY interaction winning over the Kondo interaction and may thus drive the system antiferromagnetic. A study of thermal transport under uniaxial pressure would be of great interest. Another very interesting observation was made by a polarized neutron study.[5] In applied magnetic fields a small magnetization has been observed at the Ni site, in addition to the one on the Ce sites. In magnetic fields applied along the *a* axis this magnetization is displaced towards the nearest-neighbor Ce atom. The authors ascribed this to an anisotropic and field-dependent hybridization between Ce and Ni. This might also be the origin of the unusual anisotropic field dependence of the thermopower (Fig. 2) and of the low-temperature thermal conductivity (insets of Fig. 4).

In the following we compare our data to theoretical predictions for CeNiSn available in the literature. Ikeda and Miyake[35] (IM) describe CeNiSn in the framework of the periodic Anderson model at half filling, with a hybridization matrix element that vanishes along the *a* axis, supposing a special symmetry of the crystal field ground state. The thermal conductivity resulting from the IM DOS was calculated by Moreno and Coleman[36] for the *a* axis and for the *bc* plane. $\kappa_a(T)$ has a pronounced maximum at $0.002 \times D$, where $2D$ is the bandwidth of the conduction band. $\kappa_{bc}(T)$ displays only a very moderate enhancement at this temperature, with $\kappa_a/\kappa_{bc}=2.3$. Moreno and Coleman propose that the anisotropic hybridization leading to the IM state is not driven by a particular crystal field symmetry but rather by Hund's interaction acting on virtual $4f^2$ configurations of the Ce ions. Besides the IM state, Moreno and Coleman find a quasioctahedral state (which we shall call MC state) for which the hybridization vanishes exactly along the *a* axis and vanishes almost along the (1,1) and (1,−1) directions in the *bc* plane. The thermal conductivity for this MC state is also given in Ref. 36. Here, it is $\kappa_{bc}(T)$ that has a maximum at $0.003 \times D$, while $\kappa_a(T)$ decreases continuously at this temperature. The anisotropy is with $\kappa_{bc}/\kappa_a=1.5$ at $0.003 \times D$ less pronounced than for the IM state. Our data (cf. Fig. 3) favor the MC scenario in that $\kappa_b(T)$ and $\kappa_c(T)$ show more pronounced enhancements than $\kappa_a(T)$. The agreement between the MC state and our data (cf. Fig. 3) is even better than the agreement between the MC state and the data of Ref. 20 where $\kappa_a(T)$ and $\kappa_c(T)$ showed similar enhancements. A serious shortcoming of both the IM and the MC state is, in our opinion, that they yield transport properties which are isotropic in the *bc* plane, which is clearly not the case (cf. Figs. 1 and 3). The major open problem, however, is the discrepancy between our interpretation of the enhancements in $\kappa(T)$ as *phonon-dominated* features and the theoretical calculations yielding similar enhancements for the *purely electronic* contribution to $\kappa(T)$.

Finally, we discuss the temperature dependence of the reduced Lorenz number L/L_0 of CeNiSn, where L is the Lorenz number $\kappa/(\sigma T)$ and L_0 its Sommerfeld value 2.45×10^{-8} $W\Omega/K^{-2}$. σ is the electrical conductivity. For a simple metal $L/L_0=1$ at low temperatures where the thermal conductivity is entirely electronic in nature and charge carriers are scattered (elastically) from static lattice defects. In Fig. 5 we plot L/L_0 of our *a*-axis CeNiSn crystal as a function of temperature between 100 mK and 7 K. L/L_0 decreases from 18 at 7 K to 1.48 at 100 mK. The large values at high temperatures are in agreement with our prior interpretation that in this temperature range κ is phonon dominated. The saturation below 200 mK to a constant value indicates that, below 200 mK, the thermal conductivity is entirely electronic in origin, confirming that there is a finite metallic DOS at the Fermi level. However, the value 1.48 to which L/L_0 saturates, is distinctly enhanced over 1. There are several possibilities for such an enhancement to occur. A first interpretation uses the apparent semimetal-like character of CeNiSn. In an intrinsic semiconductor, generation of electron-hole pairs at the hot sample end and recombination (with emission of an energy of the order of the gap energy) at the cold sample end lead to an additional contribution to the thermal conductivity and therefore to enhanced L/L_0 values. As indicated in Ref. 37 one expects an analogous effect in semimetals. A second explanation considers the many-body interactions in CeNiSn. In the framework of the Anderson-impurity model, Cox[38] has calculated L/L_0 and found values between 1.2 and 2 at temperatures above the coherence temperature T_0. Below T_0, however, L/L_0 tends to the value 1. For the scattering time figuring in the expressions for the transport coefficients, Cox used the Abrikosov-Suhl resonance lacking ''fine structure,'' as typical for a single impurity. This is, of course, only a very rough approximation of the real situation in CeNiSn, especially at low temperatures where the pseudogap is believed to open in the quasiparticle DOS. It would be of great interest to calculate the temperature dependence of L/L_0, possibly for all three crystallographic directions, using the more realistic quasiparticle DOS (Refs. 35, 36, and 39) proposed for CeNiSn.

V. SUMMARY

Our low-temperature measurements of the thermopower and the thermal conductivity along the a, b, and c axes of high-quality CeNiSn single crystals are in agreement with an energy pseudogap opening along all three directions somewhat below 10 K and being strongly reduced by magnetic fields applied along the a axis. Below 300 mK, the thermal conductivity along all three directions is a linear function of temperature providing strong evidence for a residual charge-carrier density existing within the pseudogap, for all three directions. The large anisotropic structures in the temperature dependence of the thermopower suggest that the charge-carrier distribution around the Fermi level is anisotropic and has sharp temperature-dependent features, even at the lowest temperatures where the pseudogap is believed to have completely opened. The unusual field dependences of the structures in $S(T)$ at approximately 1 K and of the low-temperature thermal conductivity might indicate that the magnetic field leads to a redistribution of the residual charge-carrier density in k space. The relation between this possible charge redistribution and the suppression of the pseudogap remains to be established. Calculations of the transport coefficients using the existing models for CeNiSn would definitely further enhance the current understanding of CeNiSn.

ACKNOWLEDGMENTS

We gratefully acknowledge useful discussions with P. Thalmeier, who brought Refs. 37 and 38 to our attention, with A. Freimuth, A. Hiess, and E. Kaul. We thank K. Maezawa for his valuable advice for the solid-state electrotransport technique. The work at Hiroshima was supported in part by a Grant-in-Aid for Scientific Research from the Ministry of Education, Science, and Culture of Japan and by the NEDO International Joint Research Grant.

[1] R. V. Skolozdra, O. E. Koretskaya, and Y. K. Gorelenko, Inorg. Mater. (Transl. of Neorg. Mater.) **20**, 520 (1984).
[2] T. Takabatake, Y. Nakazawa, and M. Ishikawa, Jpn. J. Appl. Phys., Suppl. 3 **26**, 547 (1987).
[3] G. Aeppli and Z. Fisk, Comments Condens. Matter Phys. **16**, 155 (1992).
[4] I. Higashi, K. Kobayashi, T. Takabatake, and M. Kasaya, J. Alloys Compd. **193**, 300 (1993).
[5] A. Hiess, I. Zobkalo, M. Bonnet, J. Schweizer, E. Lelièvre–Berna, F. Tasset, Y. Isikawa, and G. H. Lander, J. Phys.: Condens. Matter **9**, 9321 (1997).
[6] T. Takabatake, F. Teshima, H. Fujii, S. Nishigori, T. Suzuki, T. Fujita, Y. Yamaguchi, J. Sakurai, and D. Jaccard, Phys. Rev. B **41**, 9607 (1990).
[7] M. Kyogaku, Y. Kitaoka, H. Nakamura, K. Asayama, T. Takabatake, F. Teshima, and H. Fujii, J. Phys. Soc. Jpn. **59**, 1728 (1990).
[8] T. Ekino, T. Takabatake, H. Tanaka, and H. Fujii, Phys. Rev. Lett. **75**, 4262 (1995).
[9] S. Mair, H.-A. Krug von Nidda, M. Lohmann, and A. Loidl, Phys. Rev. B **60**, 16 409 (1999).
[10] K. Nakamura, Y. Kitaoka, K. Asayama, T. Takabatake, H. Tanaka, and H. Fujii, J. Phys. Soc. Jpn. **63**, 433 (1994).
[11] T. Takabatake, G. Nakamoto, T. Yoshino, H. Fujii, K. Izawa, S. Nishigori, H. Goshima, T. Suzuki, T. Fujita, K. Maezawa, T. Hiraoka, Y. Okayama, I. Oguro, A. A. Menovsky, K. Neumaier, A. Bückl, and K. Andres, Physica B **223&224**, 413 (1996).
[12] K. Izawa, T. Suzuki, T. Fujita, T. Takabatake, G. Nakamoto, H. Fujii, and K. Maezawa, Phys. Rev. B **59**, 2599 (1999).
[13] G. Nakamoto, T. Takabatake, H. Fujii, A. Minami, K. Maezawa, I. Oguro, and A. A. Menovsky, J. Phys. Soc. Jpn. **64**, 4834 (1995).
[14] G. Nakamoto, T. Takabatake, Y. Bando, H. Fujii, K. Izawa, T. Suzuki, T. Fujita, A. Minami, I. Oguro, L. T. Tai, and A. A. Menovsky, Physica B **206&207**, 840 (1995).
[15] B. Wand, Ph.D. thesis, TU Darmstadt, Germany, 1998.
[16] A. Hiess, C. Geibel, G. Sparn, C. D. Bredl, F. Streglich, T. Takabatake, and H. Fujii, Physica B **199&200**, 437 (1994).
[17] T. Takabatake, G. Nakamoto, H. Tanaka, Y. Bando, H. Fujii, S. Nishigori, H. Goshima, T. Suzuki, T. Fujita, I. Oguro, T. Hiraoka, and S. K. Malik, Physica B **199&200**, 457 (1994).
[18] J. Sakurai, Y. Takamatsu, T. Kuwai, Y. Ishikawa, K. Mori, T. Fukuhara, and K. Maezawa, Physica B **206&207**, 834 (1995).
[19] Y. Ishikawa, K. Mori, Y. Ogiso, K. Oyabe, and K. Sato, J. Phys. Soc. Jpn. **60**, 2514 (1991).
[20] M. Sera, N. Kobayashi, T. Yoshino, K. Kobayashi, T. Takabatake, G. Nakamoto, and H. Fujii, Phys. Rev. B **55**, 6421 (1997).
[21] T. Takabatake, G. Nakamoto, M. Sera, K. Kobayashi, H. Fujii, K. Maezawa, I. Oguro, and Y. Matsuda, J. Phys. Soc. Jpn., Suppl. B **65**, 105 (1996).
[22] S. Nishigori, H. Goshima, T. Suzuki, T. Fujita, G. Nakamoto, H. Tanaka, T. Takabatake, and H. Fujii, J. Phys. Soc. Jpn. **65**, 2614 (1996).
[23] E. Gratz, Physica B **237-238**, 470 (1997).
[24] T. E. Mason, G. Aeppli, A. P. Ramirez, K. N. Clausen, C. Broholm, N. Stücheli, E. Bucher, and T. T. M. Palstra, Phys. Rev. Lett. **69**, 490 (1992).
[25] H. Kadowaki, T. Sato, H. Yoshizawa, T. Ekino, T. Takabatake, H. Fujii, L. P. Regnault, and Y. Isikawa, J. Phys. Soc. Jpn. **63**, 2074 (1994).
[26] F. J. Blatt, P. A. Schroeder, C. L. Foiles, and D. Greig, *Thermoelectric Power of Metals* (Plenum, New York, 1976).
[27] G. Zwicknagl, Adv. Phys. **41**, 203 (1992).
[28] See, e.g., P. H. P. Reinders, M. Springford, P. T. Coleridge, R. Boulet, and D. Ravot, Phys. Rev. Lett. **57**, 1631 (1986); L. Taillefer and G. G. Lonzarich, *ibid.* **60**, 1570 (1988).
[29] Y. Onuki and T. Komatsubara, J. Magn. Magn. Mater. **63-64**, 281 (1987).
[30] C. Lacroix, J. Magn. Magn. Mater. **60**, 145 (1986).
[31] K. Umeo, T. Igaue, H. Chyono, Y. Echizen, T. Takabatake, M. Kosaka, and Y. Uwatoko, Phys. Rev. B **60**, R6957 (1999).
[32] R. Bermann, *Thermal Conduction in Solids* (Clarendon, Oxford, 1976).
[33] T. Takabatake, F. Iga, T. Yoshino, Y. Echizen, K. Katoh, K. Kobayashi, M. Higa, N. Shimizu, Y. Bando, G. Nakamoto, H. Fujii, K. Izawa, T. Suzuki, T. Fujita, M. Sera, M. Hiroi, K. Maezawa, S. Mock, H. v. Löhneysen, A. Brückl, K. Neumaier,

and K. Andres, J. Magn. Magn. Mater. **177-181**, 277 (1998).
[34] S. Holtmeier, C. Hinkel, M. Aigner, G. Bruls, D. Finsterbusch, B. Wolf, W. Assmus, and B. Lüthi, Physica B **230-232**, 658 (1997).
[35] H. Ikeda and K. Miyake, J. Phys. Soc. Jpn. **65**, 1769 (1996).
[36] J. Moreno and P. Coleman, Phys. Rev. Lett. **84**, 342 (2000).
[37] J. E. Parrott and A. D. Stuckes, *Thermal Conductivity of Solids* (Pion Limited, London, 1975).
[38] Cox, Ph.D. thesis, Cornell University, Laboratory of Atomic and Solid State Physics, 1985.
[39] K. A. Kikoin, M. N. Kiselev, A. S. Mishchenko, and A. de Visser, Phys. Rev. B **59**, 15 070 (1999).